Journal of Applied Fluid Mechanics, Vol. 10, No. 4, pp. 1153-1159, 2017.
Available online at www.jafmonline.net, ISSN 1735-3572, EISSN 1735-3645.
DOI: 10.18869/acadpub.jafm.73.241.26644

Numerical Analysis on the Two-Dimensional Unsteady Magnetohydrodynamic Compressible Flow through a Porous Medium

W. Pakdee[1†], B. Yuvakanit[1] and A. K. Hussein[2]

[1] *Center for R&D on Energy Efficiency in Thermo-Fluid Systems, Department of Mechanical Engineering, Faculty of Engineering, Thammasat University, Klong Nueng, Klong Lueng, Pathumtani, Thailand*
[2] *Department of Mechanical Engineering, College of Engineering, Babylon University, Babylon City, Iraq*

†*Corresponding Author Email: pwatit@engr.tu.ac.th*

(Received June 6, 2016; accepted March 8, 2017)

ABSTRACT

In the present study, the unsteady magnetrohydrodynamic (MHD) flow of compressible fluid with variable thermal properties has been numerically investigated. The electrically conducting fluid flows through a porous media channel. The uniform magnetic field is applied perpendicular to the direction of the flow. The wall is assumed to be non-conducting and maintained at two different temperatures. The thermal conductivity and viscosity of the fluid change with temperature. Sixth - Order Accurate Compact Finite Difference scheme together with the Third-order Runge-Kutta method is used to solve a set of non-linear equations. The results of the calculation are expressed in the form of the velocity and temperature at different values of the magnetic field and porosity. The proposed mathematical model and numerical methods have been validated by comparing with the results of previously published studies that the compared results reveal the same trends. The difference is due to the compressibility and property variation effects. The results showed that the magnetic field and variable properties considerably influences the flows that is compressible thereby affecting the heat transfer as well as the wall shear stress.

Keywords: Magnetic field; Porous medium; Compressible flow; Properties that change with temperature.

NOMENCLATURE

B	magnetic field strength	u	x-component velocity
c_p	heat capacity at constant P	U,F	dimensionless velocity
Ha, M	Hartmann Number	v	y-component velocity
K	permeability		
k_{eff}	effective thermal conductivity	ρ	density
η	dimensionless distance in y-direction	μ	viscosity
p	pressure	ε	porosity
R	the gas constant	σ	electrical conductivity
t	time	θ	dimensionless temperature
T	temperature	τ	dimensionless time

1. INTRODUCTION

Magnetohydrodynamic (MHD) flows involve in utilizing magnetic field for a flow control purpose. MHD has been employed for many engineering practices such as design of MHD generators, MHD pumps, cross-field accelerators, liquid-metal cooling of nuclear reactors. In addition, the MHD flows of electrically conducting fluid through porous media have wide range of applications, for example, geothermal energy technology, petroleum drillings (Mishra *et al.* 2013). In microfluidics, MHD is studied for designing micropumps for precisely producing a continuous, nonpulsating flow in complex microchannels (Qian and Bau 1998). Furthermore the magnetic field has been utilized to confine plasma within the shape of a torus in a tokamak which is a magnetic confinement device for

producing controlled thermonuclear fusion power. MHD flows of nanofluids have also been widely investigated (Mustafa *et al*. 2017; Mansour *et al*. 2016). It has been proven that magnetic force could potentially enhance heat transfer rate.

Since the MHD in porous media has extensive applications, numerous studies in this area have been conducted. Taklifi and Aghanajafi (2012) investigated the effect of MHD on steady two-dimensional laminar mixed flow about a vertical porous surface taking into account of radiation and heat generation and absorption. A power law variation of temperature along the vertical wall was assumed. The free-convection behavior of an electrically conducting fluid was investigated near a stretching sheet embedded in a non-Darcian medium. Pal and Talukdar (2010) examined buoyancy and chemical reaction effects on MHD mixed convection heat and mass transfer in a porous medium with thermal radiation and Ohmic heating. It was observed that chemical reaction and radiation reduced the skin friction coefficient whereas magnetic field decreased temperature and velocity of the flow. The problem of combined heat and mass transfer of an electrically conducting fluid in MHD natural convection adjacent to a vertical surface was analyzed, taking into account the effects of Ohmic heating and viscous dissipation (Chen 2004). The resulting governing equations are transformed using suitable transformations and then solved numerically by an implicit finite-difference technique. Emad *et al*. (2001) investigated the convective heat transfer past a continuously moving plate embedded in a non-Darcian porous medium in the presence of a magnetic field. Recently, Mabood and Ibrahim (2016) presented a numerical analysis on the effects of soret and non-uniform heat source on steady MHD non-Darcian convective flow over a stretching sheet in a dissipative micropolar fluid with radiation and chemical reaction.

The work of El-Amin focused on the combined effect of viscous dissipation and Joule heating on MHD forced convection over a non-isothermal horizontal cylinder embedded in a fluid saturated porous medium (El-Amin 2003). An inclination angle of enclosure with a presence of magnetic field is the effective parameter to control heat transfer in the enclosure. Directional effects of magnetic field on convection within an enclosure have been studied in details (Hussain *et al.* 2012; Maatki *et al* 2016). Recently, liquid metal flows in a capillary porous system (CPS) under effects of magnetic field have been investigated (Evtikhin *et al.* 2002; Buhler *et al.* 2015). This line of research is to alleviate problems of heat load and surface erosion on the plasma facing components (PFCs) such as divertors and linings (so-called first walls) of the tokamak.

Regarding MHD flows with temperature-dependent properties, the problem of unsteady laminar fully-developed flow and heat transfer of an electrically-conducting and heat-generating or absorbing fluid with variable properties through porous channels in the presence of uniform magnetic and electric fields was formulated (Chamkha 2001). The general governing equations which included such effects as magnetic field, electric field, porous medium inertia and heat generation or absorption effects were developed. A comprehensive parametric study was performed to show the effects of the Hartmann number, electric field parameter, inverse Darcy number, inertia parameter, heat generation or absorption coefficient, exponents of variable properties and the Eckert number on the solutions. Muthtamilselvan *et al*. (2014) found that the rate of heat transfer decreased with an increase in thermal conductivity. Variable permeability has more tendency to control the fluid velocity than by applying uniform permeability in the MHD non-Darcian flow over a vertical stretching surface.

The present numerical study of the two-dimensional MHD flow includes the effect of compressibility into consideration with temperature-dependent fluid's properties accounting viscosity, heat capacity and thermal conductivity. The investigation considers a channel flow that is subjected to a transverse magnetic field. Such an investigation has not been reported thus far in the literature.

2. MATHEMATICAL MODEL

The mathematical model is proposed to study two-dimensional magnetohydrodynamic heat and momentum transfer of an electrically conducting fluid through porous channel. The model takes into account of compressibility effect and variable fluid properties. The compressible fluid is subjected to transverse magnetic field. The fluid's properties: viscosity, heat capacity and thermal conductivity are assumed temperature dependent. Brinkman-Forchheimer-extended Darcy model used to describe the flow behavior incorporates boundary viscous and inertial effects (Klayborworn *et al.* 2013). Using standard symbols, the governing equations based on a Cartesian coordinate system are as follows:

2.1 Conservation of Mass

$$\frac{\partial \rho}{\partial t} + \nabla \cdot (\rho \vec{V}) = 0 \tag{1}$$

2.2 Conservation of Momentum

$$\frac{\partial (\rho u)}{\partial t} + \nabla \cdot \left(\rho u \vec{V} \right) = -\frac{\partial p}{\partial x} + \left[\frac{\partial \tau_{xx}}{\partial x} + \frac{\partial \tau_{xy}}{\partial y} \right] - \frac{\mu}{K} u - \frac{\rho}{K} \left| \vec{V} \right| u - \sigma B_0^2 u \tag{2}$$

$$\frac{\partial (\rho v)}{\partial t} + \nabla \cdot \left(\rho v \vec{V} \right) = -\frac{\partial p}{\partial y} + \left[\frac{\partial \tau_{xy}}{\partial x} + \frac{\partial \tau_{yy}}{\partial y} \right] - \frac{\mu}{K} v - \frac{\rho}{K} \left| \vec{V} \right| v \tag{3}$$

2.3 Conservation of Energy

$$\frac{\partial \rho e_t}{\partial t} + \nabla \cdot \left(\rho e_t \vec{V} \right) = \frac{\partial}{\partial x} \left(k_{eff} \frac{\partial T}{\partial x} \right) + \frac{\partial}{\partial y} \left(k_{eff} \frac{\partial T}{\partial y} \right) - \frac{\partial (up)}{\partial x} - \frac{\partial (vp)}{\partial y} + \frac{\partial (u \tau_{xx})}{\partial x}$$

$$+\frac{\partial\left(v\,\tau_{xy}\right)}{\partial x}+\frac{\partial\left(u\,\tau_{xy}\right)}{\partial y}+\frac{\partial\left(v\,\tau_{yy}\right)}{\partial y} \tag{4}$$

2.4 Stress Tensor

$$\tau_{xy}=\mu\left[\frac{\partial v}{\partial x}+\frac{\partial u}{\partial y}\right] \tag{5}$$

$$\tau_{xx}=-\frac{2}{3}\mu\nabla\cdot\vec{V}+2\mu\frac{\partial u}{\partial x} \tag{6}$$

$$\tau_{yy}=-\frac{2}{3}\mu\nabla\cdot\vec{V}+2\mu\frac{\partial v}{\partial y} \tag{7}$$

2.5 Thermal Conductivity

$$k_{eff}=\varepsilon k_{fluid}+(1-\varepsilon)k_{solid} \tag{8}$$

where

$$k_{fluid}=\frac{\mu(T)c_p}{\mathrm{Pr}} \tag{9}$$

2.6 Total Energy and Internal Energy

$$e_t=e+\frac{1}{2}\sum_{i=1}^{2}u_i^2 \tag{10}$$

where

$$e=c_pT-\frac{p}{\rho} \tag{11}$$

2.7 Ideal Gas Law

$$p=\rho RT \tag{12}$$

2.8 Viscosity and Cpecific Heat of Fluid are Functions of Temperature Based on the Following Equations

$$\mu(T)=\mu_0\left(\frac{T}{T_o}\right)^{0.7} \tag{13}$$

where

$\mu_0=1.71\times10^{-5}$ kg/m·s and

$$c_p(T)=28.11+0.1967\times10^{-2}T+$$

$$0.4805\times10^{-5}T^2-1.966\times10^{-9}T^3 \tag{14}$$

2.9 Initial and Boundary Conditions

The dimension of the two-dimensional domain is 0.0002 m × 0.001 m as shown in Fig. 1. The chosen dimension is in the order of microfluidics magnitude. Boundary conditions implemented are based on the Navier-Stokes Characteristic Boundary Conditions (NSCBC) (Pakdee and Mahaligam 2003). The temperatures of isothermal top and bottom walls are 500 K and 300 K respectively. All the walls are non-slip. Non–reflecting boundary condition is imposed at the outflow boundary. At the inlet, flow velocity (u_p) is initialized by

$$u_p=u_0\left[\cos\left(\frac{\pi}{2}\frac{y}{l}\right)\right]^2 \tag{15}$$

where the channel width l = 0.0002 m and u_0 = 1.0 m/s at temperature of 300 K. Initially, at t = 0, u = v = 0 and temperature T = 300 K for the entire domain.

Finally, solutions are rendered nondimensional according to the following relations for velocity, temperature, and distance in the y direction and time respectively as

$$\left.\begin{aligned} F\ \text{or}\ U&=\frac{u}{u_0},\quad \theta=\frac{(T-T_L)}{(T_H-T_L)}\\ \eta&=\frac{y}{l},\quad \tau=\frac{\mu t}{\rho l^2}\end{aligned}\right\} \tag{16}$$

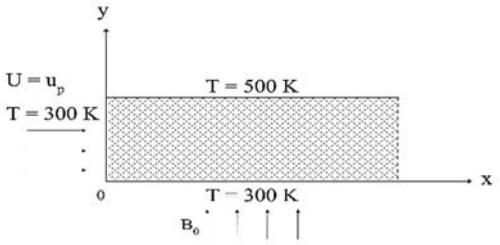

Fig. 1. Computational domain.

3. NUMERICAL PROCEDURE

The two-dimensional domain is well resolved with 129×25 grid resolution. Although the computational domain is small, the grid dependency was determined to ensure that the domain is well resolved. It was found that the temperature and velocity at the middle of the domain were less than 0.5 % when the 129×25 mesh was used. The 129×25 mesh was found to be a good compromise between computational error and computational time. The sixth - order accurate Compact Finite Difference is used to discretize the equations. The third–order Runge –Kutta method is used to advance solutions in time.

4. RESULTS AND DISCUSSION

The model proposed and numerical method are validated against the work of Chamkha (1996) in which the mathematical model for flow and heat transfer of the MHD flow through a porous medium channel is developed. In this previous work, the electrically conducting fluid is considered incompressible with constant properties. The graphical results depicting effects of Hartmann number on the flow velocity are compared for the validation purpose and shown in Fig. 2 in which the Hartmann number (M) is defined as the ratio of magnetic force to viscous force given by

$$\left(Bl\sqrt{\frac{\sigma}{\mu}}\right). \tag{17}$$

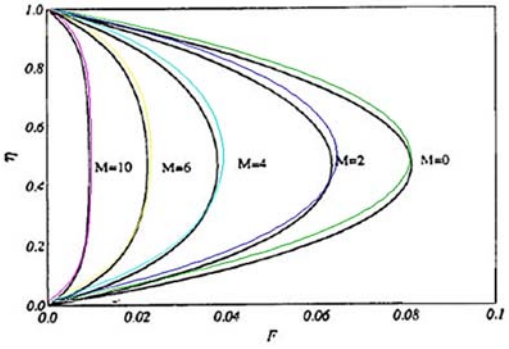

Fig. 2. Non-dimensional velocity *F* at various Hartmann number M. Black lines represent the previous work (Chamkha 1996) and pastel lines represent the present work.

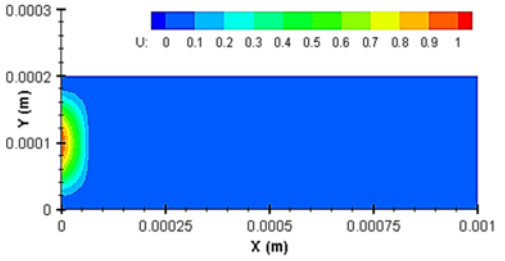

(a)

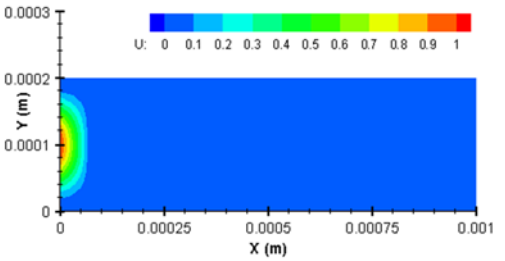

(b)

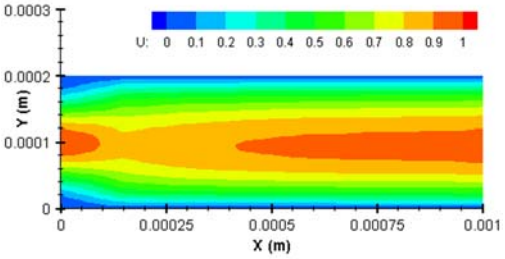

(c)

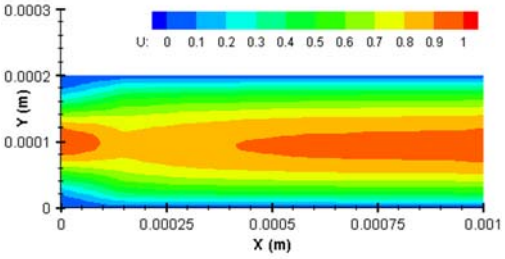

(d)

Fig. 3. Velocity fields at different times τ (a) 0.0 (b) 0.3 (c) 0.5 (d) 1.5.

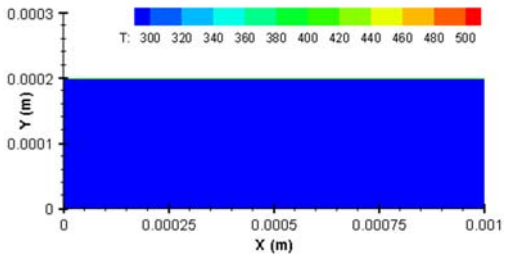

(a)

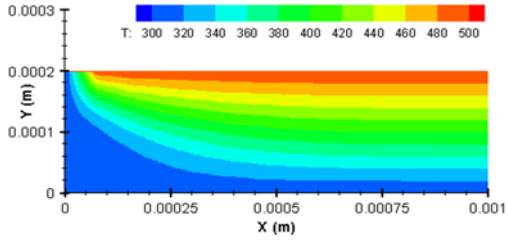

(b)

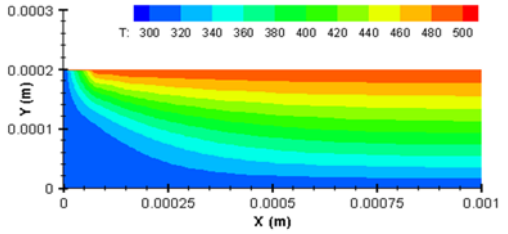

(c)

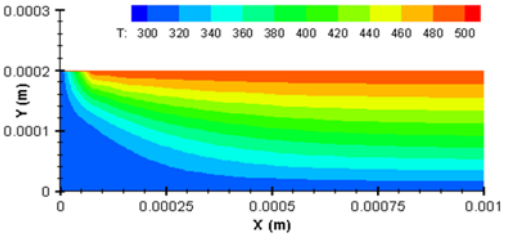

(d)

Fig. 4. Temperature fields at different times τ (a) 0.0 (b) 0.3 (c) 0.5 (d) 1.5.

The overall results appear to be in an excellent agreement. The difference is due mainly to the effects of compressibility and fluid properties. It is interesting that the peaks of velocity do not occur on the centerline of the channel. Instead, the peak locations appear to shift slightly towards the upper domain. This result is attributed to lower fluid density towards the top boundary thus the flow accelerates obeying the continuity. In this paper, the electrical conductivity σ of 3×10^{-15} S/m, permeability K of 0.001 and solid thermal conductivity k_{solid} of 0.6 W/m K are considered. Porosity of the domain is 0.7.

The computed data are extracted at various times. Distributions of velocity and temperature that evolve with time are shown in Figs. 3 and 4 respectively. Both the field variables appear to develop and achieve a steady state fast. Velocity is maximum around the center of channel. Heat is being transferred downwards from the top to bottom boundaries. Temperature gradients exhibit in two directions. The temperature gradients are higher near the upper left corner of the

domain where the warm and cold walls meet.

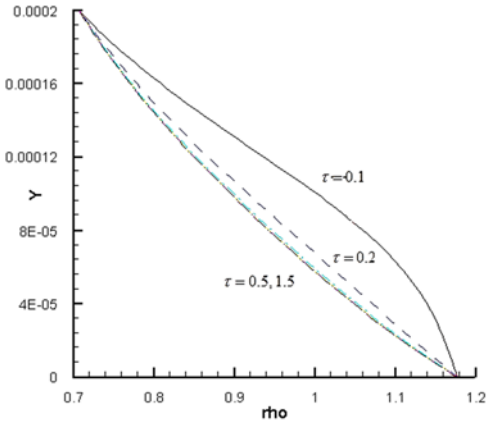

Fig. 5. Distributions of fluid density at the center of the *x*-plane at different times.

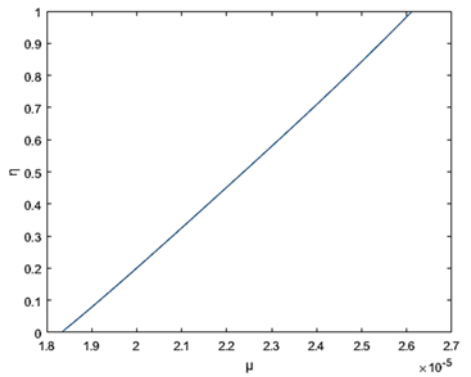

(a)

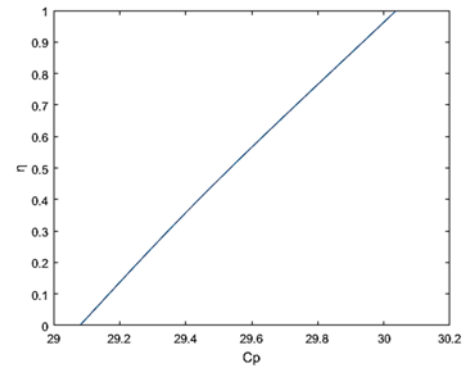

(b)

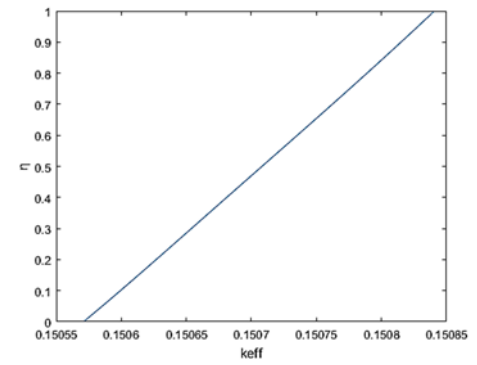

(c)

Fig. 6. Temperature−dependent properties (a) μ (b) c_p (c) k_{eff} vs. η.

In what follow, the solutions are then generalized by being transformed into dimensionless forms. Variations of the fluid density with time and space are evident in Fig. 5. The density that changes with both space and time are resulted from the temperature change. This density variation supports the results found in Fig. 2. Property profiles of viscosity specific heat and thermal conductivity with respect to vertical distance are shown in Fig. 6. The data at the midplane are extracted after steady state is reached (τ = 1.0). The values increase with temperature towards the top boundary. Variations are found nearly linear. This result is expected since the nonlinear effect appear to be small in the functions given by the Eqs. (9), (13) and (14).

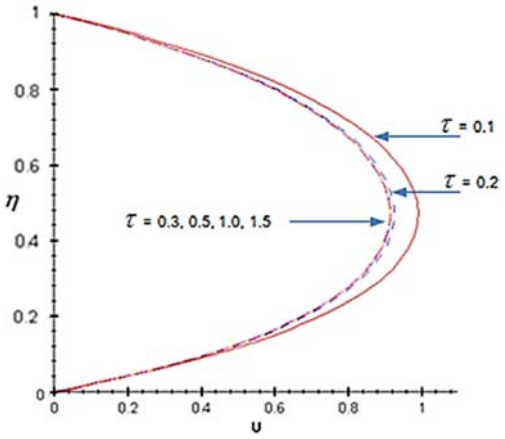

(a)

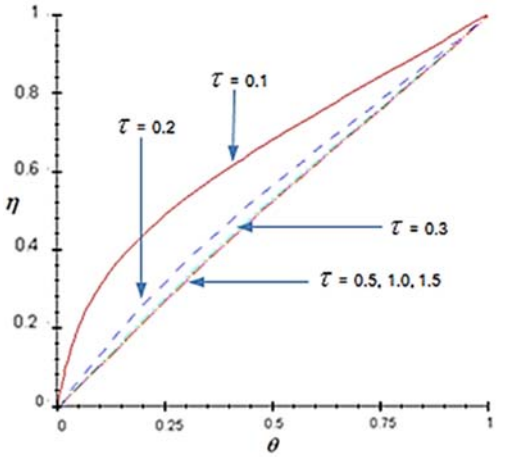

(b)

Fig. 7. Time evolution of (a) dimensionless velocity and (b) dimensionless temperature at the center of the *x*-plane.

Figure 7 illustrates the time evolution of the dimensionless velocity and temperature at the center of the *x*-plane. It is evident that the steady state is achieved rapidly from the dimensionless time equals 0.3 onwards. This result confirms what is found earlier in Figs. 2 and 3. The dimensionless temperature is fixed at 1 and 0 at the top and bottom walls, respectively. At early times, the high temperature gradient near the top wall drives heat to transfer towards the bottom wall. As approaching

steady state, temperature gradients become nearly equal throughout the domain.

Effects of magnetic strength in terms of the Hartmann number (Ha) on the flow pattern are shown in Fig. 8. The dimensionless velocity that varies with η at the half of the domain in the x-direction is investigated. As Ha increases, the Lorentz force induced by magnetic field increases. The Lorentz force, which opposes the flow, leads to enhanced deceleration of the flow around the center of the channel causing the peak value of velocity to decrease. However, the flow velocities away from the centerline increase allowing the fluid mass to conserve.

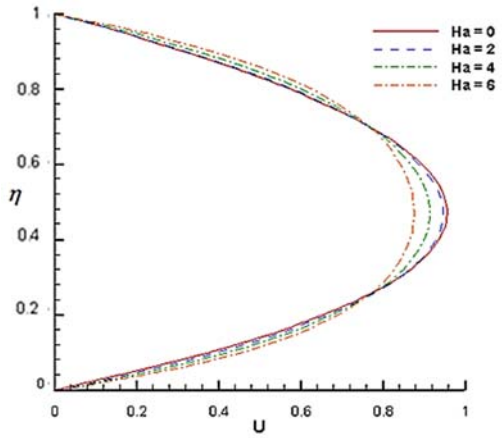

Fig. 8. Velocity profile at the center of domain for various values of Ha.

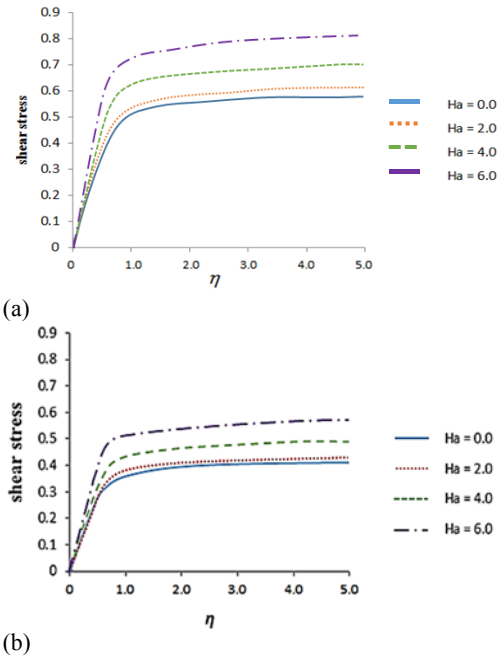

(a)

(b)

Fig. 9. The wall shear stress for various Ha values at (a) the top surface and (b) the bottom surface.

The effect of Ha on the shear stress at the top and bottom walls are depicted in Fig. 9. It can be seen that the higher magnetic field strength increases the wall shear stress due to an increase in velocity gradient at the wall. The top-wall shear stress is found greater than that at the bottom wall since velocity gradients over the upper domain are larger than those over the lower domain. This corresponds well to the velocity profiles observed earlier in Fig. 7.

5. CONCLUSION

The transient magnetrohydrodynamic (MHD) two-dimensional flow of compressible fluid with variable thermal properties has been numerically investigated. The electrically conducting fluid flows through a porous media channel subjected to transverse magnetic field. The wall is assumed to be non-conducting and maintained at two different temperatures. The thermal conductivity and viscosity of the fluid change with temperature. Favorable comparisons of the proposed mathematical model and numerical methods with previously published work are achieved. The results showed that the magnetic field, compressibility and variable fluid's properties considerably affect the heat and fluid transports. In addition, variations of density with temperature causes the asymmetric velocity profile.

ACKNOWLEDGEMENT

This work is financially supported by the Thailand Research Fund under contract number RSA 58800031. Additionally the authors would like to acknowledge Mr. Pornthep Wattanavanitkul for some post processing of the data.

REFERENCES

Buhler, L., C. Mistrangelo. and T. Najuch. (2015). Magnetohydrodynamic flows in porous structures, *Fusion Engineering and Design* 98, 1239–1243.

Chamkha, A. J. (1996). Steady and transient magnetohydrodynamic flow and heat transfer in a porous medium channel, *Fluid/Particle Separation Journal* 9(2), 129–135.

Chamkha, A. J. (2001). Unsteady laminar hydromagnetic flow and heat transfer in porous channels with temperature-dependent properties, *International Journal of Numerical Methods for Heat & Fluid Flow* 11(5), 430-448.

Chen, C. H. (2004). Combined heat and mass transfer in MHD free convection from a vertical surface with Ohmic heating and viscous dissipation, *International Journal of Engineering Science* 42, 699–713.

El-Amin, M. F. (2003). Combined effect of viscous dissipation and Joule heating on MHD forced convection over a non-isothermal horizontal cylinder embedded in a fluid saturated porous medium, *Journal of Magnetism and Magnetic Materials* 263, 337–343.

Emad, M., M. S. Abo-Eldahab and E. I. Gendy (2001). Convective heat transfer past a continuously moving plate embedded in a non-Darcian porous medium in the presence of a magnetic field, *Canadian Journal of Physics* 79.

Evtikhin, V. A. I. E. Lyublinski, A. V. Vertkov, S. V. Mirnow, V. B. Lazarev and N. P. Petrova (2002). Lithium divertor concept and results of supporting experiments, *Plasma Physics and Controlled Fusion* 44, 955.

Hussain, H. S., A. K. Hussein and R. N. Mohammed (2012). Studying the effects of a longitudinal magnetic field and discrete isoflux heat source size on natural convection inside a tilted sinusoidal corrugated enclosure, *Computers and Mathematics with Applications* 64, 476-488.

Klayborworn, S., W. Pakdee, P. Rattanadecho and S. Vongpradubchai (2013). Effects of material properties on heating processes in two-layered porous media subjected to microwave energy, *International Journal of Heat and Mass transfer* 61, 397-408.

Maatki, C., Ghachem, K. Aissia, H. B. Hussein, A. K. Borjini, M. N. and H. B. Aissia (2016). Inclination effects of magnetic field direction in 3D double-diffusive natural convection, *Applied Mathematics and Computation* 273, 178-189.

Mabood, F. and S. M. Ibrahim (2016). Effects of soret and non-uniform heat source on MHD non-Darcian convective flow over stretching sheet in a dissipative micropolar fluid with radiation, *Journal of Applied Fluid Mechanics* 9, 2503-2513.

Mansour, M. A., S. E. Ahmed and A. M. Rashad (2015). MHD natural convection in a square enclosure using nanofluid with the influence of thermal boundary conditions, *Journal of Applied Fluid mechanics* 9, 2515-2525.

Mishra, S. R., G. C. Dash and M. Acharya (2013). Mass and heat transfer effect on MHD flow of a visco-elastic fluid through porous medium with oscillatory suction and heat source, *International Journal of Heat and Mass Transfer* 57(2), 433-438.

Muthtamilselvan, M., D. Prakash and D. H. Doh (2014). Effects of non-uniform heat generation on unsteady MHD non-Darcian flow over a vertical stretching surface with variable properties, *Journal of Applied Fluid Mechanics* 7, 425-434.

Pakdee, W. and S. Mahalingam (2003). Accurate Method to Implement Boundary Conditions for Reacting Flows Based on Characteristic Wave Analysis, *Combust .Theory and Modelling* 7, ٧٠٥–712.

Pal, D. and B. Talukdar (2010). Buoyancy and chemical reaction effects on MHD mixed convection heat and mass transfer in a porous medium with thermal radiation and Ohmic heating, *Commun Nonlinear Sci Numer Simulat* 15, 2878–289.

Qian, S. and H. Bau (1998) Magneto-hydrodynamics based microfluidics, *Mechanics Research Communications* 36 (1), 10–21.

Taklifi, A. and C. Aghanajafi (2012). MHD non-Darcian flow through a non-isothermal vertical surface embedded in a porous medium with radiation, *Meccanica* 47, 929–937.